Easterly wave disturbances over Northeast Brazil: an observational analysis

Hindawi Publishing Corporation
Advances in Meteorology
Volume 2015, Article ID 176238, 20 pages
http://dx.doi.org/10.1155/2015/176238

Research Article

Easterly Wave Disturbances over Northeast Brazil: An Observational Analysis

Helber Barros Gomes,[1] Tércio Ambrizzi,[1] Dirceu Luís Herdies,[2] Kevin Hodges,[3] and Bruce Francisco Pontes da Silva[4]

[1] *Institute of Astronomy, Geophysics and Atmospheric Sciences, University of São Paulo, 05508-090 São Paulo, SP, Brazil*
[2] *CPTEC-INPE, 12630-000 Cachoeira Paulista, SP, Brazil*
[3] *NERC Centre for Earth Observation, University of Reading, Reading RG6 6BB, UK*
[4] *Capixaba Institute of Research, Technical Assistance and Rural Extension, 29052-010 Vitoria, ES, Brazil*

Correspondence should be addressed to Helber Barros Gomes; gomes.helber@gmail.com

Received 19 January 2015; Revised 8 May 2015; Accepted 11 May 2015

Academic Editor: Luis Gimeno

This paper aims to identify the circulation associated with Easterly Wave Disturbances (EWDs) that propagate toward the Eastern Northeast Brazil (ENEB) and their impact on the rainfall over ENEB during 2006 and 2007 rainy seasons (April–July). The EWDs identification and trajectory are analyzed using an automatic tracking technique (TracKH). The EWDs circulation patterns and their main features were obtained using the composite technique. To evaluate the TracKH efficiency, a validation was done by comparing the EWDs number tracked against observed cases obtained from an observational analysis. The mean characteristics of EWDs are 5.5-day period, propagation speed of ~9.5 m·s^{-1}, and a 4500 km wavelength. A synoptic analysis shows that between days −2 d and 0 d, the low level winds presented cyclonic relative vorticity and convergence anomalies both in 2006 and 2007. The EWDs signals are strongest at low levels. The EWDs propagation is associated with relative humidity and precipitation positive anomalies and OLR and omega negative anomalies. The EWDs tracks are seen over all ENEB and their lysis occurs between the ENEB and marginally inside the continent. The tracking captured 71% of EWDs in all periods, indicating that an objective analysis is a promising method for EWDs detection.

1. Introduction

Northeast Brazil (NEB, Figure 1) is located at the eastern extreme of tropical South America, approximately between latitude 1°–18°S and longitude 35°–48°W, with an area exceeding 1.6 million km^2. The NEB is subject to various meteorological systems that induce rainfall with large temporal and spatial variability. However, while the east coast receives around 1600 mm annual rainfall, some inland dry regions receive less than 750 mm [1]. This variability coupled with high temperatures throughout the year is responsible for the semiarid climate in the region.

It is possible to identify three different rainfall regimes in NEB [2–4]. In the northern NEB, the main rainy season occurs from February to May and can be linked to the Intertropical Convergence Zone (ITCZ), which reaches its southernmost position during March-April [5]. In the southern NEB, the rainy season occurs from December to February and is associated with cold front (CF) incursions that reach low latitudes [2]. The NEB east coast has its rainy season from April to July and, according to [2, 6], is mainly due to sea breeze circulations, above all overnight, and Cfs or their remnants occurring along the coast. In addition, [7, 8] also suggested that this maximum is related to Easterly Wave Disturbances (EWDs), which propagate westward over the tropical South Atlantic Ocean during the austral autumn and winter.

The EWDs are disturbances that move westward with the trade winds associated with the subtropical ridges. According to [9], the position and intensity of the South Atlantic ridge are an important mechanism for the low-level water vapor transport toward NEB. These disturbances are important

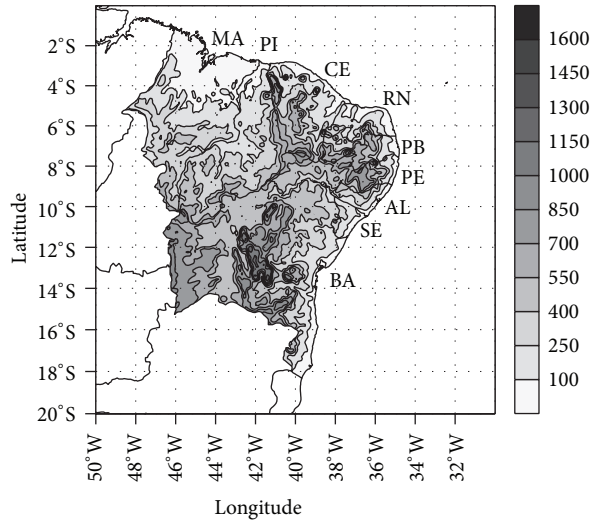

Figure 1: Northeast Brazil geographical location and study area. The orography is depicted by shading (m).

climatologically because they carry large amounts of moisture to areas that are typically dry. When EWDs interact with local circulations, low-level convergence can be increased, sometimes resulting in increased rainfall over the eastern and northern NEB coasts.

Several studies have shown that EWDs occur in various tropical regions, mainly in the western Pacific Ocean, Caribbean Sea, West Africa, and eastern Atlantic Ocean [10–25]. In the South Atlantic tropical region, near the Brazilian cost, EWDs can also occur, though less frequently than elsewhere [8, 26–32].

The study of [27] considered the kinematic characteristics of tropical synoptic disturbances over the South Atlantic at 700 hPa and showed that they are generally very weak when compared to those in the Northern Hemisphere, especially in May to August. These disturbances typically have periods of 3–5 days. The study of [27] also suggested that African easterly waves could cross the Atlantic Ocean and contribute to organized convection over South America. The study of [32] analyzed two EWD events that reached the NEB eastern coast on May 15, 2005, and June 20, 2006. They found that areas with large convective activity were associated with upward motion and humidity convergence regions at low levels. Although the EWDs in the NH are often associated with a Low Level Jet (LLJ), for example, the African Easterly Jet or the Caribbean jet [22], this mechanism does not appear to be a factor in the South Atlantic, though further investigation is still necessary.

Recently, [30] performed a detailed study of the relationship between westward positive unfiltered relative vorticity over the southern tropical Atlantic, Mesoscale Convective System (MCS) occurrences over the western southern tropical Atlantic and strong rainfall events (anomaly $> 10\,\text{mm}\cdot\text{day}^{-1}$) over the NEB eastern coast. Their results suggested that ocean-atmosphere processes are responsible for the strong precipitation episodes and a significant percent of the rainfall episodes were associated with EWD events.

The rainfall produced by EWDs benefits society in tropical South America in terms of agriculture and power generation, but they are also often responsible for flash floods, landslides in high risk areas, and erosion. There is still little knowledge of the physical and dynamical mechanisms involved in the development and maintenance of EWDs and their variability in this region. Thus, the main objective of this paper is to identify the circulation patterns generated by the movement of EWDs to the NEB eastern coast (hereafter called ENEB) and their importance for the total rainfall over this region during the 2006 and 2007 rainy seasons. Additionally, we will analyze the identification and trajectory of these disturbances using an automatic tracking technique.

2. Data and Methods

2.1. Data Sets. The data used here are from the European Centre for Medium-Range Weather Forecasting (ECMWF) interim reanalysis (ERAI; [33–35]). The ERAI is the latest global atmospheric reanalysis produced by the ECMWF and is a continuation of their production of reanalyses following on from the previous atmospheric reanalysis ERA-40 [36]. The meteorological fields used in the analysis are horizontal fields of relative vorticity, streamlines, humidity, and temperature at the pressure levels 1000, 850, 700, 600, 500, 400, 300, and 200 hPa and vertical profiles of temperature, humidity, and vertical velocity along the latitude 8°S. These data are available on a $1.5^\circ \times 1.5^\circ$ grid from 1979 to the present at 4 times' daily resolution, although we will only consider here the years 2006 and 2007. More years will be considered for a following paper about the climatology of EWDs. In addition to ERAI data, daily mean outgoing longwave radiation (OLR) data from the National Oceanic and Atmospheric Administration (NOAA) polar-orbit meteorological satellites, on a regular grid of $2.5^\circ \times 2.5^\circ$ resolution [37] and precipitation from the Tropical Rainfall Measuring Mission (TRMM) on a $0.25^\circ \times 0.25^\circ$ grid [38] are used. To verify the cloud and synoptic systems associated with EWDs, the Meteosat 7 satellite images in the visible (0.5–0.9 μm), water vapor (5.7–7.1 μm), and infrared (10.5–12.5 μm) channels are used.

2.2. Composite Analysis. The EWD average circulation patterns were obtained using the composite technique. The observed cases of EWDs that reached NEB were obtained from [31] subjective analysis. The EWD events were initially detected in Meteosat infrared satellite images with a 3 hours' temporal resolution by considering the cloudiness and characteristic disturbance scale, that is, synoptic and subsynoptic, which moved westward over the tropical south Atlantic throughout the study period. From the first detection step (cloudiness identification), [31] selected the events as potential EWDs. The second and final detection step was to analyze relative vorticity and streamline fields at 1000, 850, 700, 500, and 200 hPa using the ERAI data in order to find typical EWD circulation patterns, in accordance with the definitions in the literature. Those systems with the above characteristics were classified as EWDs. The analysis indicates the occurrence of 26 (22) systems in the rainy season of April to July (AMJJ) in 2006 (2007) which are listed in Table 1. The

Table 1: Observed EWDs dates to the 2006 and 2007 rainy season (AMJJ) (left columns) and tracked by TracKH (right columns).

2006		2007	
Date	Track	Date	Track
29/Mar.–03/Apr.	Ok	04–06/Apr.	—
07–09/Apr.	Ok	07–14/Apr.	Ok
13–15/Apr.	—	14–21/Apr.	—
21–23/Apr.	Ok	24–29/Apr.	Ok
21–27/Apr.	Ok	25/Apr.–02/May	Ok
21/Apr.–02/May	Ok	27/Apr.–04/May	Ok
13-14/May	Ok	14–16/May	—
15–17/May	Ok	17–19/May	—
21–23/May	Ok	18–22/May	Ok
21–25/May	—	20–24/May	—
28–31/May	—	28/May–01/Jun.	Ok
02–06/Jun.	—	02–04/Jun.	Ok
08–13/Jun.	Ok	06–09/Jun.	Ok
13–18/Jun.	Ok	07–13/Jun.	Ok
19–22/Jun.	Ok	14–17/Jun.	Ok
22–26/Jun.	—	24–30/Jun.	Ok
25–28/Jun.	Ok	27/Jun.–02/Jul.	—
27-28/Jun.	—	03–05/Jul.	Ok
05–07/Jul.	Ok	11–13/Jul.	Ok
06–12/Jul.	—	21–24/Jul.	Ok
12–14/Jul.	—	24–27/Jul.	Ok
14–16/Jul.	Ok	27–29/Jul.	—
14–19/Jul.	Ok		
18–20/Jul.	Ok		
16–23/Jul.	Ok		
22–28/Jul.	Ok		

choice of these two years, within the period of five years from [31], was taken to evaluate the variability from one year with EWD events with less convective activity (2006) against a year with more convective activity (2007). A detailed analysis using the composite method is first carried out before seeing how the objective tracking performed. Composite maps for the days in which EWDs were observed were generated for 2 days prior to the event day (i.e., when the EWDs have reached the ENEB), the event day, and 2 days following the event (−2 d, 0 d, and +2 d, resp.).

2.3. Tracking Technique. The current knowledge of the EWD life cycle, including genesis, growth, and dynamical aspects, is still limited. Thus, an automatic objective analysis method is explored to identify and track the EWDs. This method was developed by [39, 40] (TracKH) and has been widely applied to analyze African Easterly Waves (AEW) [15, 22, 24], which are usually more intense and have been more extensively studied compared to waves in the Southern Hemisphere (SH) [27]. The main differences in the EWDs between the hemispheres are their intensity and distance traveled [24, 41].

TracKH identifies and tracks EWDs that exceed a relative vorticity threshold and requires that this threshold meets certain lifetime and distance traveled requirements. In previous studies, the relative vorticity was initially smoothed to a T42 resolution (~280 km grid spacing at the equator) using a spectral transform based on spherical harmonics that, according to [24], is adequate to identify this kind of wave (synoptic) and reduces the relative vorticity noise at higher resolutions. The reduced resolution is used to remove the very small subsynoptic spatial scales, which can result in multiple vorticity centres and/or subsynoptic phenomena centres, which can lead to tracking errors [42]. Although the TracKH has been widely used in many regions, particularly over the African continent and North Atlantic, it has not been applied to the tropical South Atlantic, near NEB. The identification and tracking criteria of EWDs used in this region were modified from [24]. For this study, EWDs identification uses a T63 resolution and a threshold vorticity of -0.5×10^{-5} s^{-1} with systems identified as minima lower than the threshold. We also required systems to travel at least 500 km (~5°) and persist for at least 1.5 days. These changes were necessary because the amplitude of the EWDs is usually lower in the SH when compared to the NH. Genesis and lysis density are also derived from the tracking method, where the first (last) point in each track is considered as a genesis (lysis) location. The densities are computed as the number of track, genesis, or lysis points per month per unit area (~10^6 km^2) using the spherical kernel method [43].

In order to evaluate the efficiency of the TracKH method, each relative vorticity centre tracked (dates and paths) was compared with the EWDs identified by [31].

3. Results

3.1. Synoptic and Dynamic Analysis of EWDs. The atmospheric circulation patterns that could help to identify the EWD activity over ENEB are discussed in this section. Composites of atmospheric variables were made for times with and without EWDs during the 2006 and 2007 rainy seasons (AMJJ) for two days before (−2 d) until two days after (+2 d) the event day. The composite anomalies were computed for the same periods using arithmetic differences between the composites with and without EWDs with the aim of amplifying the signal.

The EWDs were identified using satellite image analysis and 700 hPa wind composite fields. The EWDs presented an average of 5 days duration between detection and dissipation both for 2006 and 2007, according to the satellite image analysis. Using the 700 hPa composite fields, the EWDs average lifetime and wavelength are 5.5 days and 4500 km (45°), respectively. The mean phase velocity was 9.5 m s^{-1}. These characteristics are close to those found by [8, 27, 44]. The individual years are considered next.

(a) 2006 Rainy Season. Figure 2 shows the relative vorticity (RV) and streamline composite anomalies for the 2006 rainy season at 1000 hPa (left column), 850 hPa (center column), and 700 hPa (right column) for the −2 d to +2 d times. The dashed lines show the approximate trough axes. On day −2 d, at 1000 hPa (Figure 2(a)), an anomalous cyclonic circulation

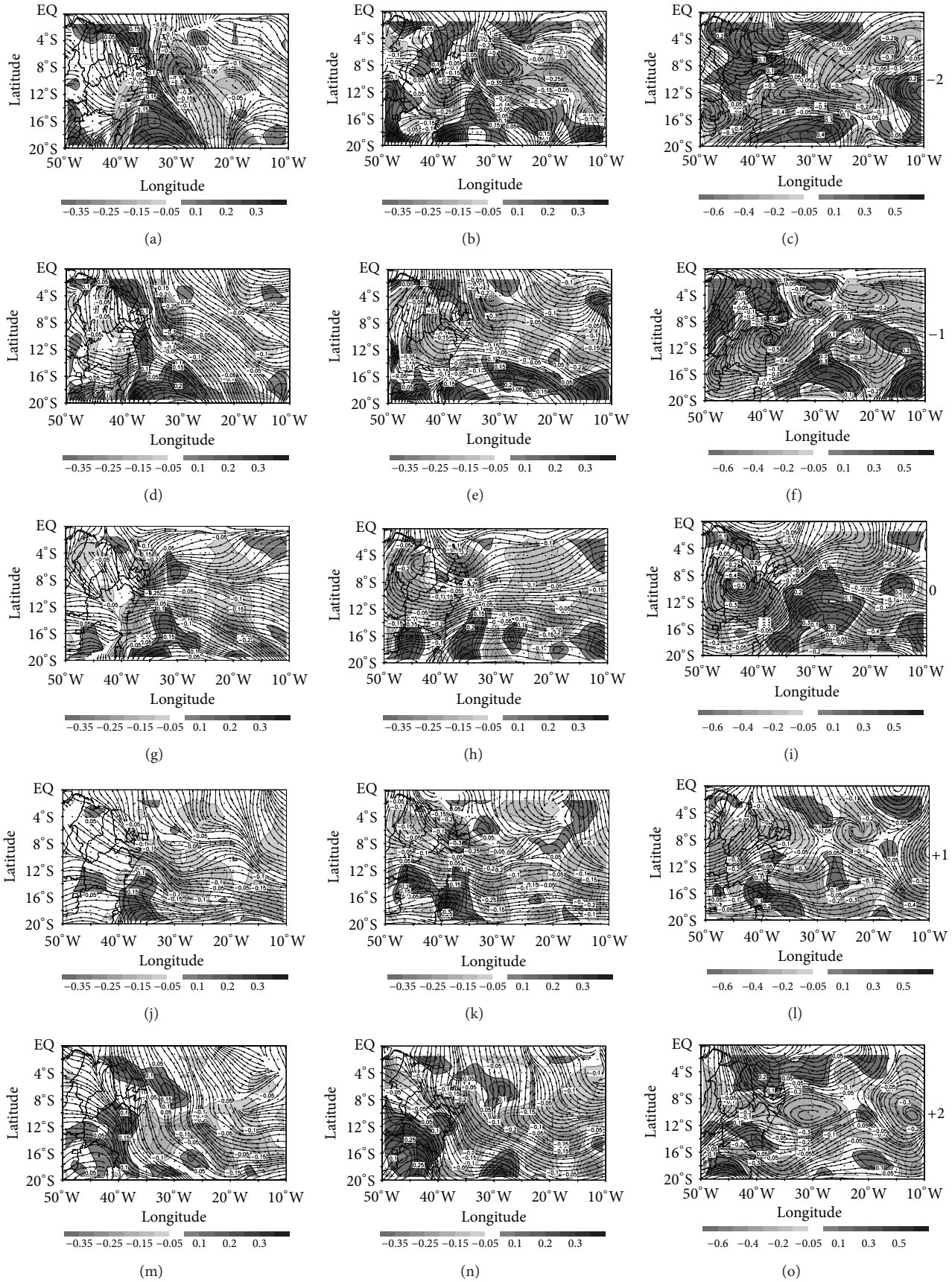

Figure 2: Relative vorticity (shaded, 10^{-5} s^{-1}) and streamlines composite anomalies in the period from April to July 2006 at 1000 hPa (left column), 850 hPa (center column), and 700 hPa (right column). The approximate trough axis is shown by dashed line.

is observed with RV minima as low as $-0.35 \times 10^{-5}\ s^{-1}$ in the Tropical South Atlantic (TSA) (~9°S–29°W) linked to EWD propagation. At 850 hPa (Figure 2(b)), this anomaly was also identified but with a more intense cyclonic circulation and RV minima ($-0.4 \times 10^{-5}\ s^{-1}$), but located further east (~1°) relative to that at 1000 hPa. At the 700 hPa level (Figure 2(c)) there is instead only an anomalous trough (dashed line) connected to a RV minima centre of about $-0.2 \times 10^{-5}\ s^{-1}$. The study of [26] identified the layer with highest occurrence of EWDs throughout the entire year. Their results showed that the highest frequency of EWDs occurs in the 850–700 hPa layer during the rainy season, in accordance with the results presented here.

Between days −2 d and −1 d the wind and RV anomalies associated with EWDs move westward, approaching the ENEB at all levels. At day 0 d (Figures 2(g)–2(i)) the troughs and RV minima associated with the EWDs reach the ENEB on all levels, but with greater intensity at 850 hPa (as low as $-0.35 \times 10^{-5}\ s^{-1}$), favoring upward motion. This feature also was obtained on day +1 d between 850–700 hPa. On day +2 d (Figures 2(m)–2(o)) no anomaly pattern associated with EWDs was identified.

Figure 3 shows the horizontal divergence composite anomalies for the 2006 rainy season at 1000 hPa (left column), 850 hPa (center column), and 700 hPa (right column). On day −2 d, at 1000 hPa (Figure 3(a)), an anomalous convergence centre associated with EWDs is observed with a value of $-0.3 \times 10^{-5}\ s^{-1}$ (9°S–27°W) in phase with the circulation and anomalous cyclonic vorticity patterns identified in Figure 2(a) (day −2 d). At 850 hPa (Figure 3(b)), there is a convergence anomaly associated with EWDs, but with lower intensity (as low as $-0.1 \times 10^{-4}\ s^{-1}$) compared to the 1000 hPa level. A positive anomaly (divergence) is detected at 700 hPa (Figure 3(c)). This suggests that there is an inversion in the convergence/divergence pattern between 1000 and 700 hPa. According to [20], the EWD propagation is associated with mass convergence (divergence) at low (medium/high) levels of the atmosphere. The study of [45] determined the mean structure of 13 EWDs in ENEB (June 3 to July 27, 1994) and found that the convergence dominates from the surface to 800 hPa. They also suggested that the convergence maximum at low levels might be explained by the interaction of north/east winds acting perpendicular to the coast, while south/southeast winds reach this same region parallel to the coast. The centres identified on day −2 d associated with EWDs propagate westward and reach the ENEB on day 0 d (Figures 3(g)–3(i)), with increased intensity. In the following days there is no evidence of any convergence/divergence anomalies over this region.

In order to evaluate how the EWDs change through the troposphere, vertical cross sections of the composite anomalies along 8°S (Figure 4) of the relative humidity (%, left column), vertical velocity ($m\,s^{-1}$, center column), and temperature (°C, right column) were examined. This latitude was chosen by considering the intensity of the EWDs and the most affected areas according to the observational analysis.

On day −2 d a centre of anomalous relative humidity (Figure 4(a)) (and upward motion, Figure 4(b)), associated with EWDs, of up to 4% ($-2\ m{\cdot}s^{-1}$) centered at approximately 28°W (26°W) and between the 950–650 hPa (1000–600 hPa) levels is observed. Over the ENEB coast, there is a predominance of downward motion, no significant humidity anomalies and negative temperature anomalies at all levels. At day −1 d, the moisture (Figure 4(d)) and upward motion (Figure 4(e)) anomalies intensify and propagate westward associated with a positive temperature anomaly centre between 700–500 hPa. The EWDs reach ENEB on day 0 d according to the anomaly fields, indicated by the presence of positive moisture (Figure 4(g)) anomalies (upward movement, Figure 4(h)) in the lower and middle levels of about 8% ($-3\ m{\cdot}s^{-1}$). In addition, a layer of positive temperature anomalies at 700–500 hPa is identified between two layers of negative anomalies.

Figure 5 shows the TRMM precipitation (left column) and convection (right column, negative values) associated with EWDs. It is observed that on day −2 d (Figures 5(a) and 5(b)) a positive precipitation (negative) anomaly (Outgoing Longwave Radiation, OLR) occurs between the longitudes 25°–30°W and latitudes 6°–12°S. On day −1 d (Figures 5(c) and 5(d)) these anomalous centres propagate westward and reach the ENEB on day 0 d (Figures 5(e) and 5(f)) along with the negative RV centres and convergence presented in Figures 2 and 3. The precipitation close to the ENEB on days −2 d and −1 d is weak. However, as the EWDs approach, precipitation becomes intense (up to $5\ mm{\cdot}day^{-1}$) over ENEB, especially along the coastlines of AL, PE, RN, and PB states (see Figure 1). The OLR indicates that the EWDs are characteristically shallow, but it is possible to identify them by their negative OLR anomalies up to two days before and until day 0 d. On day +1 d (Figures 5(g) and 5(h)) one can still see positive precipitation anomalies associated with EWDs over ENEB. From the precipitation and OLR anomalies positive (negative) precipitation (OLR) anomalies are also seen over BA southern/eastern coast, which is probably associated with other types of system.

The main synoptic features associated with EWDs during the 2006 season were obtained through the analysis of composites from two days before until two days after their impact on ENEB. In summary, these results indicate the movement of cyclonic vorticity and convergence anomalies at low levels from the east over the TSA until they reach ENEB. Furthermore, we highlight the moisture and upward motion between low and middle levels associated with EWDs. These anomalies agree with the OLR and precipitation anomalies, especially at day 0 d (Figures 5(e) and 5(f)).

(b) 2007 Rainy Season. The wind and RV anomalies associated with EWDs for the 2007 rainy season are shown in Figure 6. These anomalies are computed at the levels 1000, 850, and 700 hPa for days −2 d until +2 d and indicate as before the westward propagation of the EWDs. The cyclonic anomaly is in phase with the trough and the anticyclonic centre is south of it. In 2006 (Figure 2), the anticyclonic RV anomaly had a less intense signal than in 2007. This is probably due to the reduced convective observed in that season. On day 0 d (Figures 6(g)–6(i)) it can be seen that the trough and RV cyclonic anomaly are present (as low as $-5 \times 10^{-4}\ s^{-1}$)

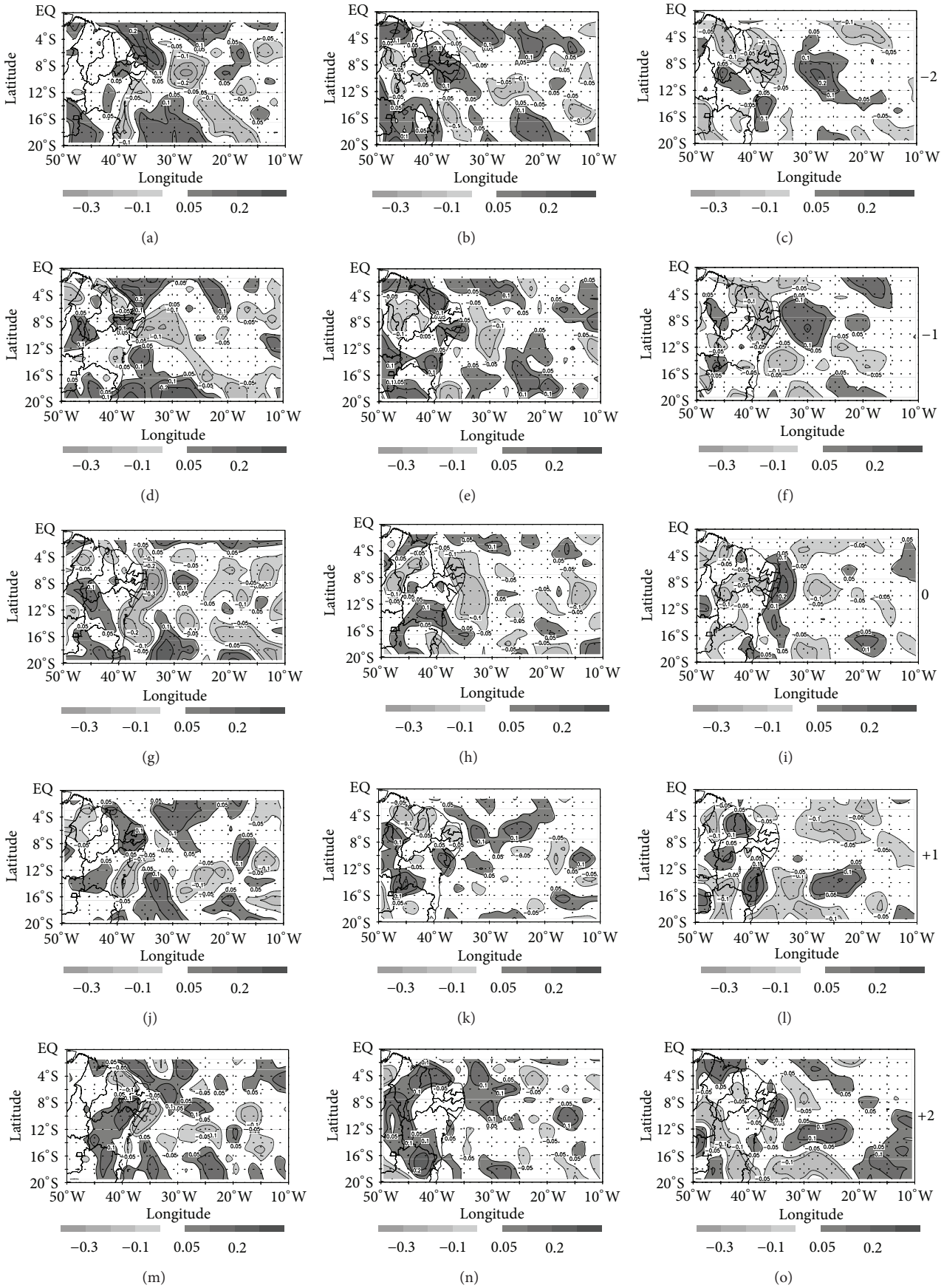

Figure 3: As in Figure 2, but for the horizontal divergence (10^{-5} s^{-1}).

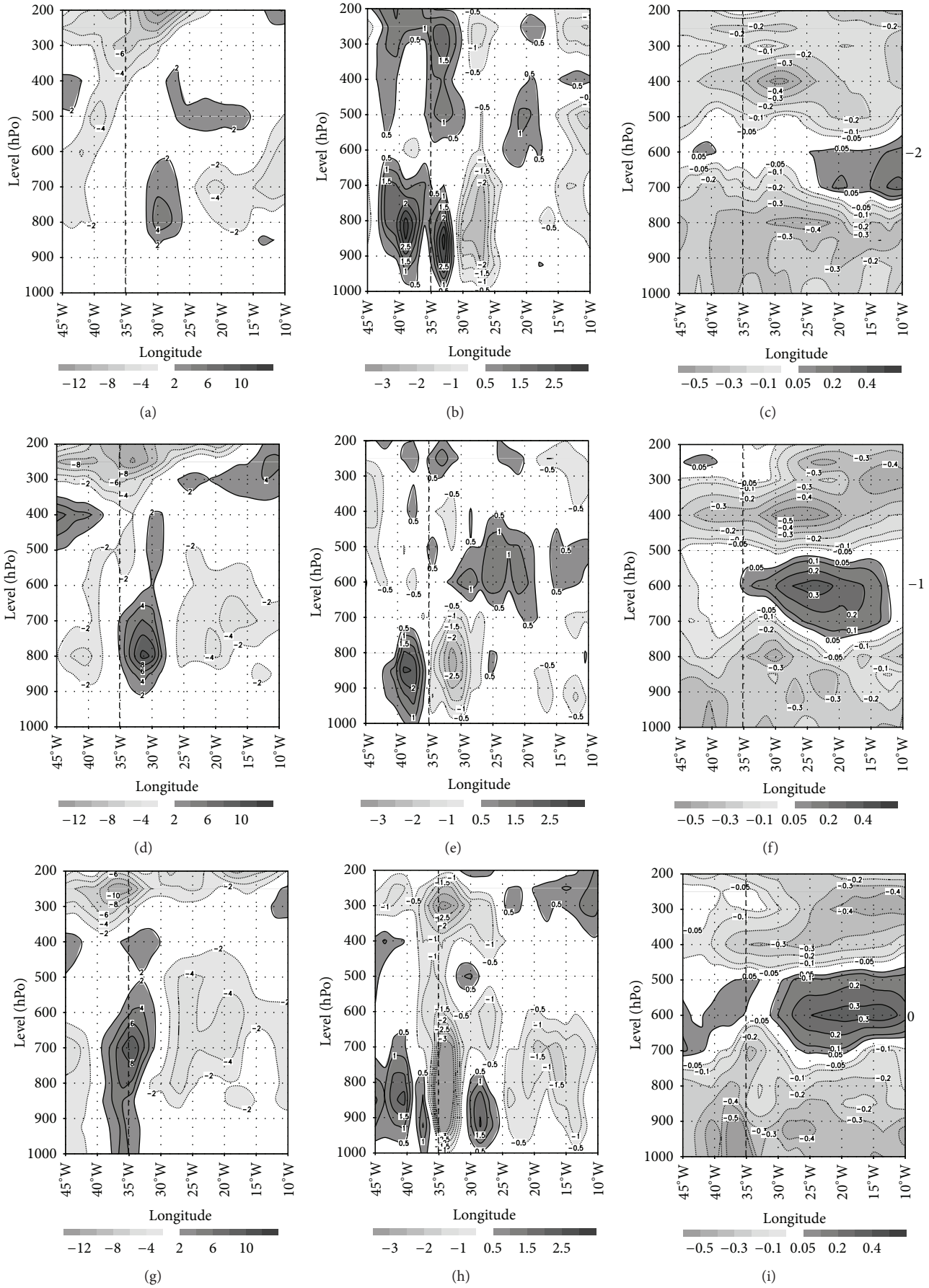

Figure 4: Continued.

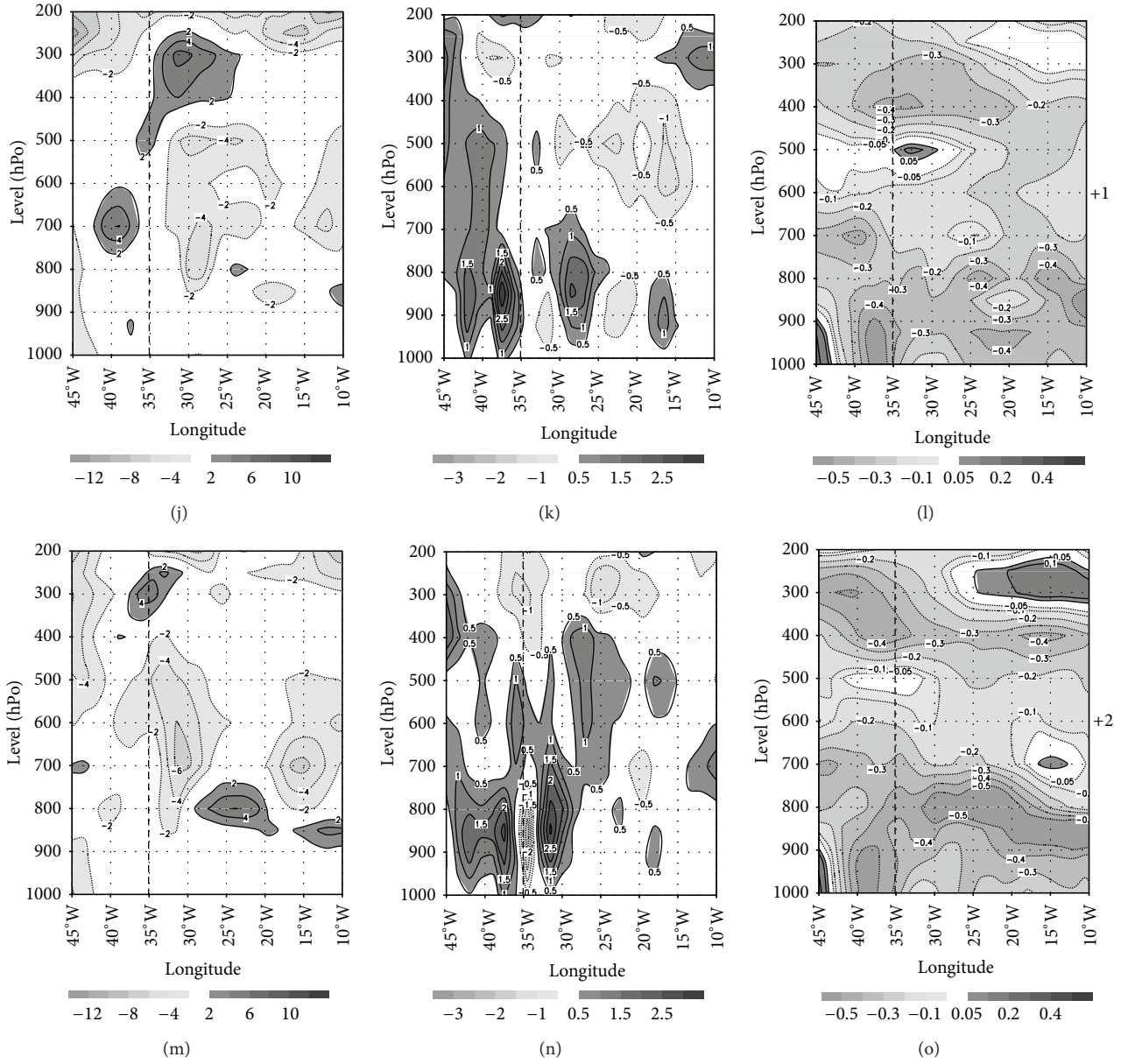

Figure 4: Vertical cross-sections composite anomalies along 8°S of the relative humidity (%, left column), vertical velocity ($m \cdot s^{-1}$, center column), and temperature (°C, right column) in the period from April to July 2006. The vertical dashed line at 35°W mark the subjectively estimated longitudinal position of littoral ENEB.

in all the chosen levels over the ENEB. These anomalies are more intense compared to the 2006 rainy season as well as influencing all the NEB coast.

The horizontal divergence anomalies (Figure 7) show convergence centres associated with EWDs for all days at 1000 and 850 hPa. At 700 hPa (right column), the opposite pattern is identified, similar to the results of the 2006 (Figure 3) rainy season, which also showed divergent anomalies at this level from day −2 d until +2 d. Furthermore, the convergence centres obtained in 2007 are more intense than those observed in 2006 at all levels. On the other hand, the 850 hPa (Figure 7, center column) convergence anomalies in 2006 (Figure 3) rainy season are seen better. In addition, we highlight the positive anomaly pattern (divergent) south of the negative anomaly as discussed in Figure 6.

Figure 8 shows the vertical cross section composite anomalies along 8°S of the relative humidity (left), vertical velocity (middle), and temperature (right) during the 2007 rainy season. On day −2 d a relative humidity anomalous centre (8%, Figure 8(a)) is identified between 900–400 hPa associated with upward motion (Figure 8(b)) of about $-1.5\ m \cdot s^{-1}$. On subsequent days these anomalous centres move westward growing stronger over ENEB (dashed line) on day 0 d (Figures 8(g) and 8(h)). The EWDs impact on ENEB is observed at day 0 d at all levels. The 2006 rainy season (Figure 4) has these anomalies confined between lower and middle levels.

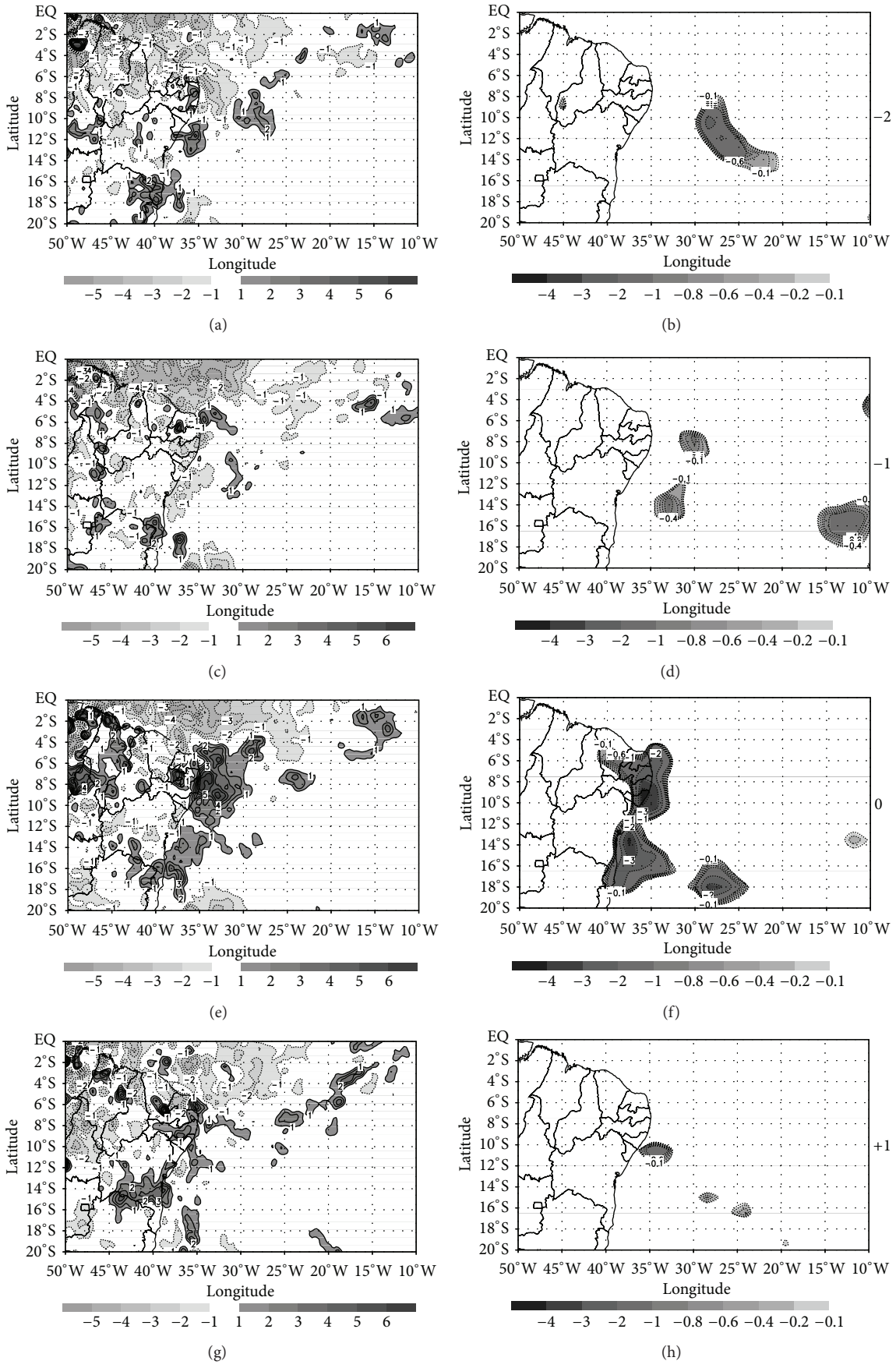

Figure 5: Continued.

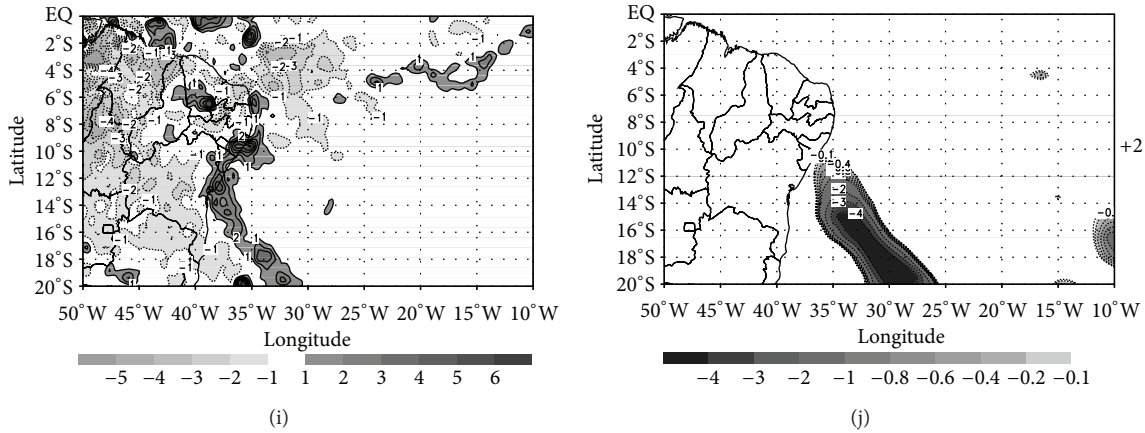

FIGURE 5: Precipitation (left column, mm·day^{-1}) and outgoing longwave radiation (right column, W·m^{-2}) composite anomalies in the period from April to July 2006.

Furthermore, it can be observed that on day +1 d there is a relative humidity anomaly (Figure 8(j)) between longitudes 35° and 40°W, while the upward motion (Figure 8(k)) is restricted to 750 hPa. On day +2 d these anomalies are reduced but they still have an influence over ENEB. For the temperature anomalies (Figure 8, right column), note on day −2 d (Figure 8(c)) a positive anomaly centre between 1000 and 900 hPa with negative anomalies above (850–400 hPa). On day −1 d these centres move westward and there is a new positive centre between 700 and 500 hPa to the rear. The following day (Figure 8(i)), the ENEB is influenced by negative anomalies at almost all layers, except between the 950 and 800 hPa levels which shows positive anomalies. On day +1 d there is a slight temperature increase at midlevels while on day +2 d this anomalous heating is more pronounced. These temperature anomalies are consistent with the composites of the other variables, which showed EWDs more intense in 2007 when compared to 2006.

The precipitation and OLR anomalies for the 2007 rainy season are shown in Figure 9. From day −2 d the negative (positive) OLR (precipitation) anomalies associated with EWDs are clearly identified propagating westward through to day 0 d (Figures 9(e) and 9(f)), as well as their influence over ENEB with an intensity of about −4 W·m^{-2} (6 mm·day^{-1}). In 2006, these anomalies had a lower intensity but were better identified on day 0 d (Figures 5(e) and 5(f)) compared to 2007. Furthermore, it is observed that the EWDs contribute to the precipitation over ENEB on days +1 d and +2 d, with maxima along the AL and RN coastline. In the 2006 season, this influence was noted until day +1 d (Figures 5(g) and 5(h)) with more variable spatial distribution.

In summary the synoptic features associated with EWDs for the 2007 season are similar to the 2006 period, but having more intense anomalies. These anomalous patterns were noted for all composite days propagating westward with a major influence over ENEB at day 0 d.

3.2. EWDs Tracking: Statistics and Validation. In this section, the main life cycle of EWDs features are discussed in terms of genesis, track, and lysis densities. The EWD events in the TSA seem to be better identified when TracKH is applied at the 850 hPa level, where the relative vorticity centres are most intense. Although the EWDs are better captured at 850 hPa using the vorticity, the trough associated with them can be found from 1000 up to 700 hPa, at least. However, only the 850 hPa analysis results are presented.

TABLE 2: Percentage of EWDs detected by TracKH, EWDs tracks, and other systems cyclonic vorticity centre tracks.

Period	2006	2007	Average
% EWD detected	73	68	71
% tracks with EWD	48	38	43
% of others systems	52	62	57

Table 1 shows the dates of EWDs that reached ENEB according the subjective detection of [31] and the events detected by TracKH during the 2006 and 2007 rainy seasons (AMJJ). In the first (second) period, 26 (22) EWDs were identified by [31], while the TracKH detected 40 relative vorticity centre trajectories in both periods (80 in total), of which 19 (15) coincided with the ones detected by the observational analysis of [31]. From these results, it was determined that the percentage of EWDs detected by TracKH (Table 2) that coincided with those identified by [31] were 73% and 68% in 2006 and 2007, respectively.

Due to the travel distance criterion used, some EWDs that intensified closer to the ENEB were not captured. The average percentage of the observed EWDs detected by TracKH was about 71% (Table 2), but the number of events tracked (80 events) is higher than those observed (48 events). The vorticity centres associated with EWDs were separated from the other centre types tracked by TracKH. Table 2 indicates that 43% (34 vorticity centres) tracked by TracKH are EWDs and 57% (46 vorticity centres) represent vorticity minima associated with other weather systems, such as perturbations produced in the trade winds, Cfs or their remnants and ITCZ. These systems will be investigated further in future work.

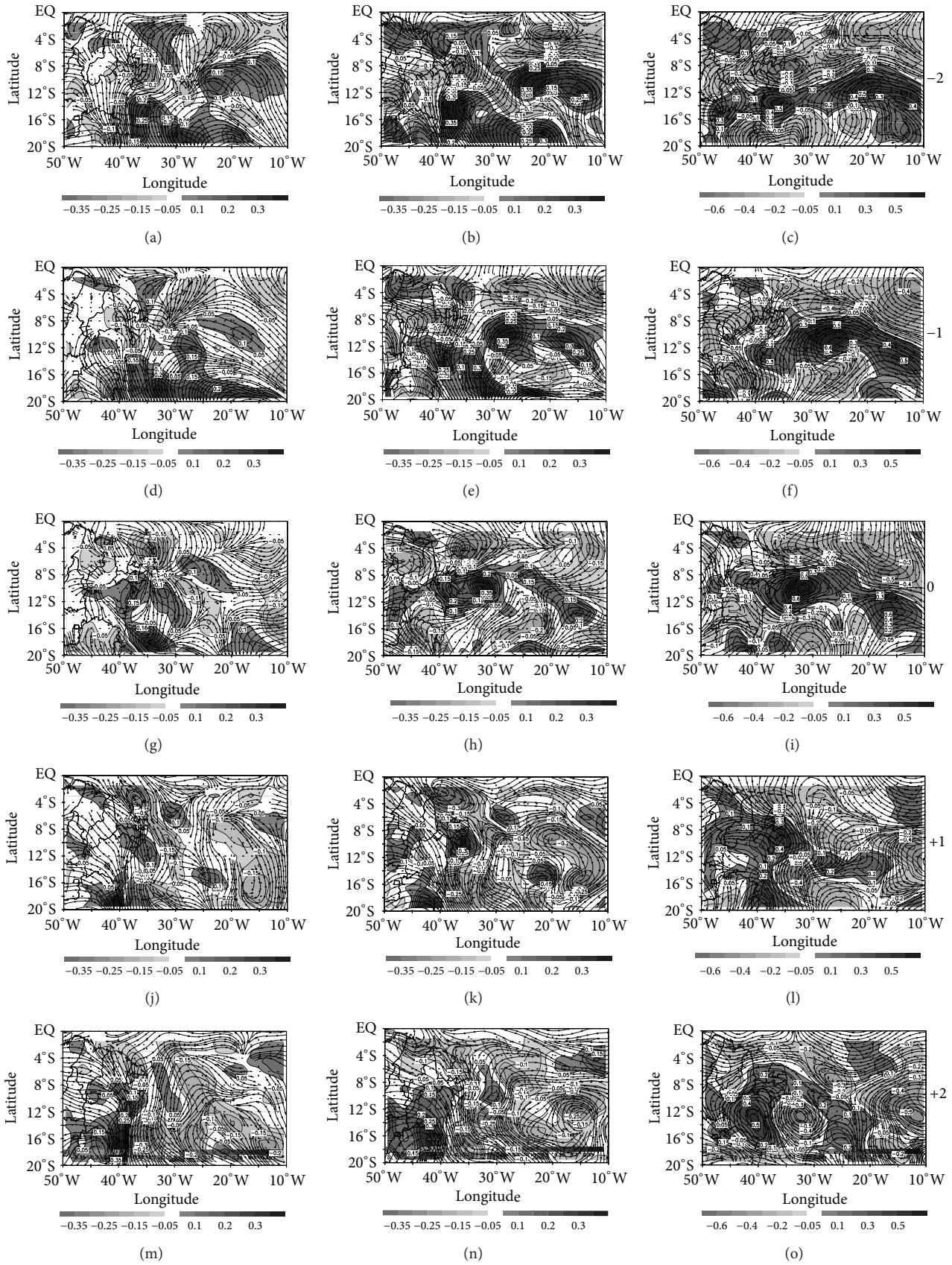

Figure 6: Relative vorticity (shaded, 10^{-5} s^{-1}) and streamlines composite anomalies in the period from April to July 2007 at 1000 hPa (left column), 850 hPa (center column), and 700 hPa (right column). The approximate trough axis is shown by dashed line.

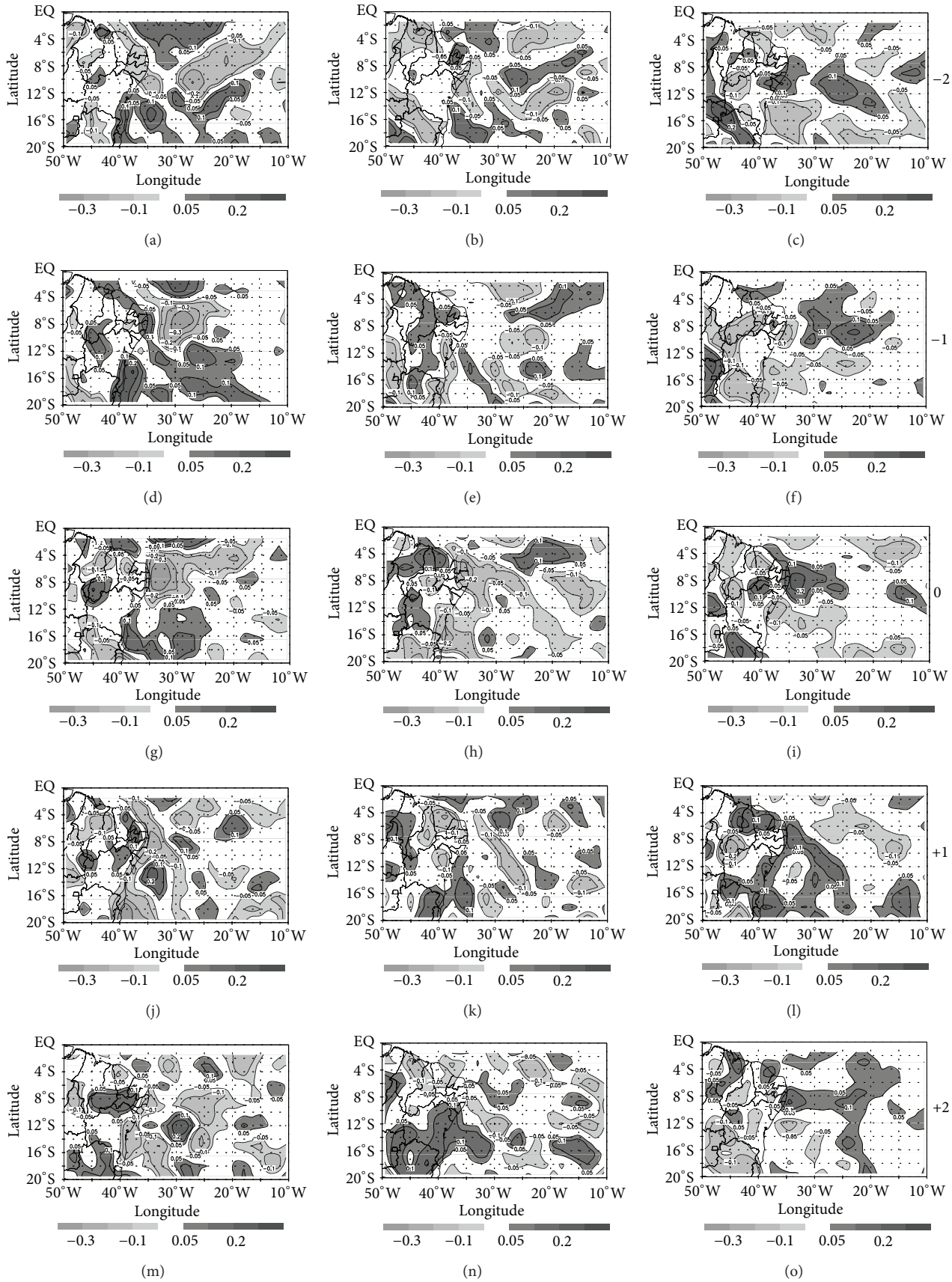

Figure 7: As in Figure 6, but for the horizontal divergence (10^{-5} s^{-1}).

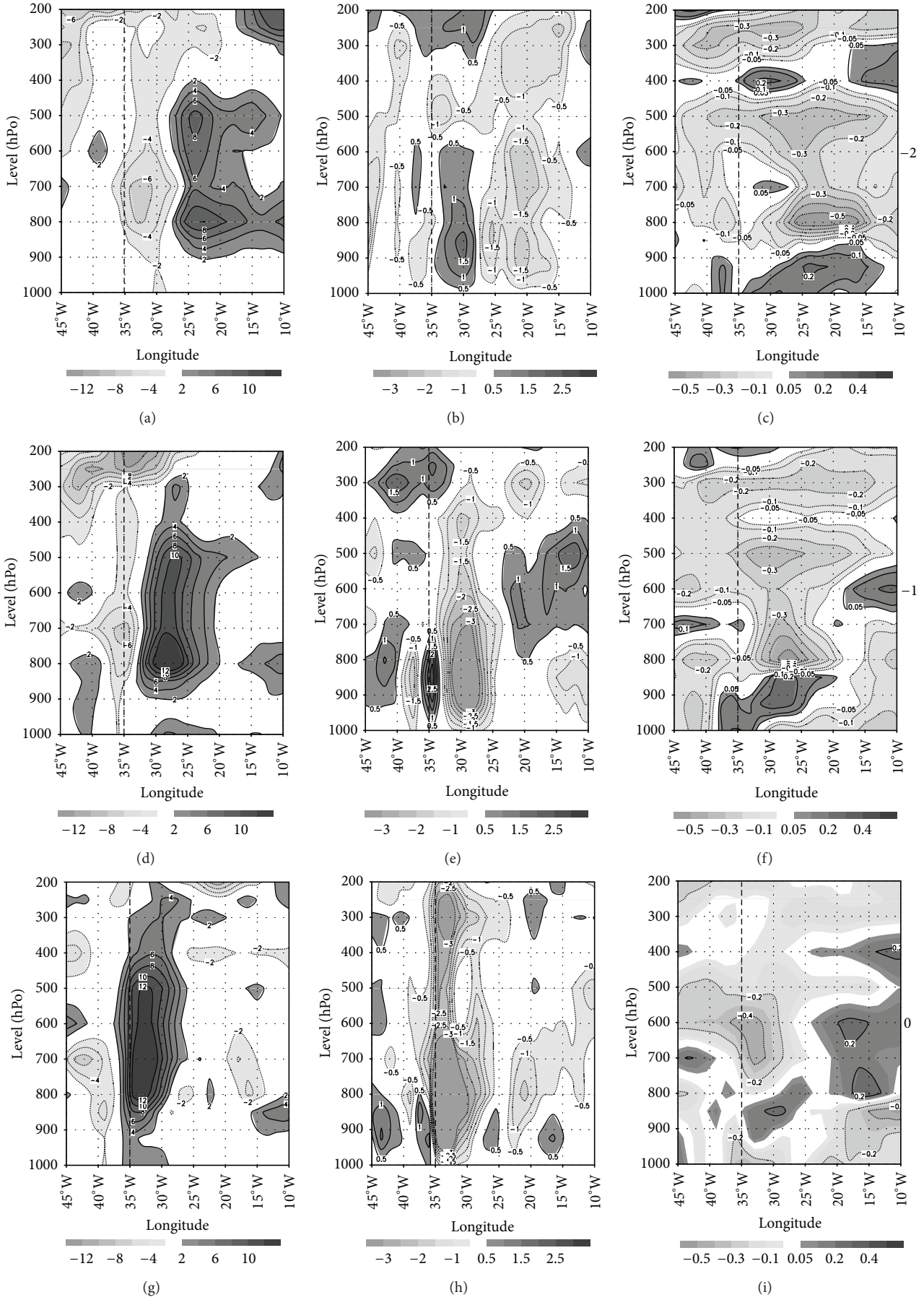

Figure 8: Continued.

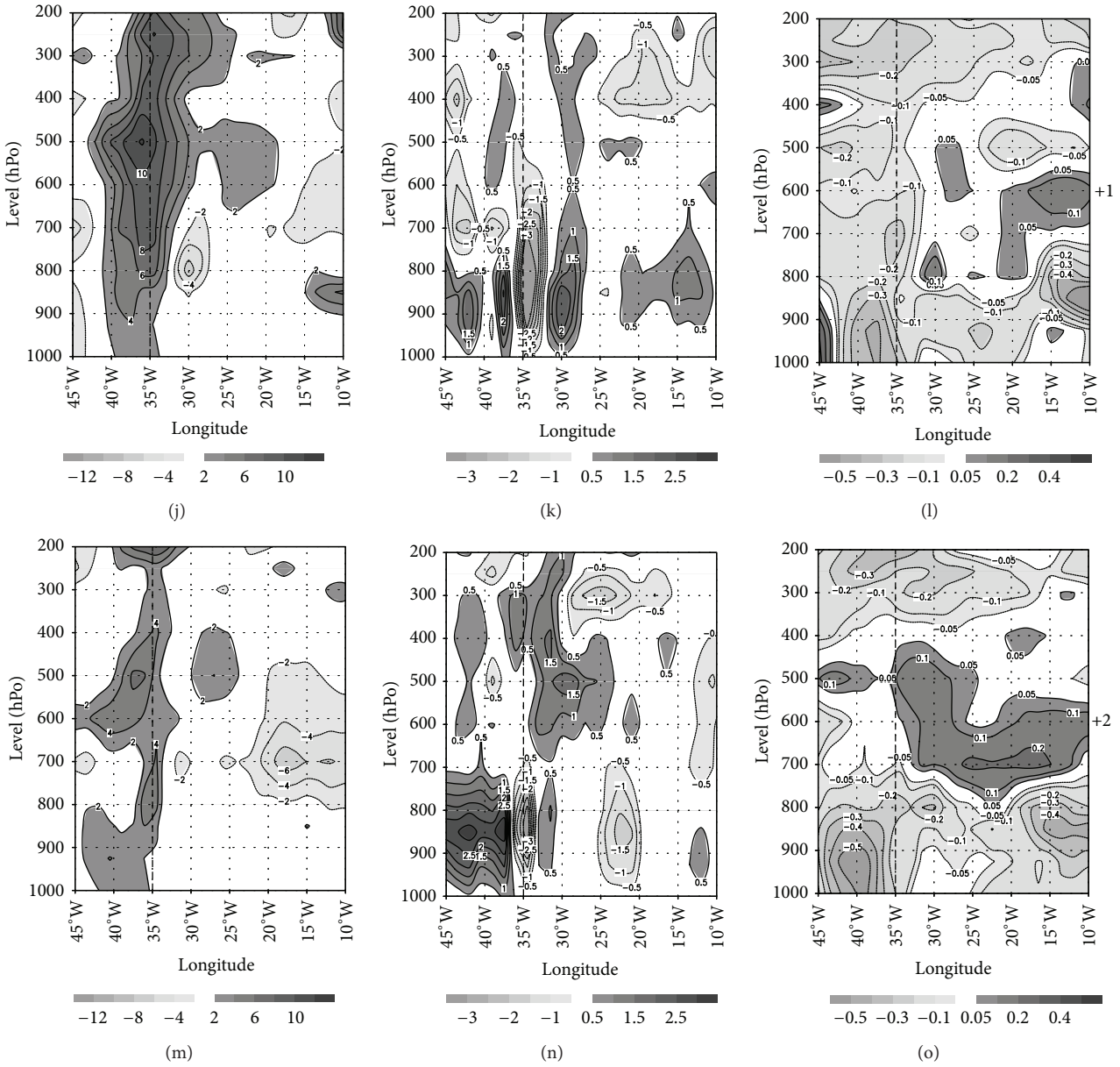

Figure 8: Vertical cross-section composite anomalies along 8°S of the relative humidity (%, left column), vertical velocity (m·s^{-1}, center column), and temperature (°C, right column) in the period from April to July 2007. The vertical dashed line at 35°W mark the subjectively estimated longitudinal position of littoral ENEB.

Figures 10(a) and 10(b) show the April–July cyclonic vorticity tracks for 2006 and 2007 in 850 hPa, respectively. In 2006, most of the tracks could be detected over both NEB eastern and northern coasts. However, northern trajectories are parallel and far from the coastal line when compared to the eastern tracks (perpendiculars to the coast). The 2007 rainy season, in contrast, had a less EWDs activity around the ENEB and more trajectories parallel to the NEB northern coast. Over the ENEB, only 3 events were observed.

Knowledge of the life cycle of EWDs over ENEB is still unclear, mainly due to a lack of understanding of their interaction with other weather systems. According to [21, 46], the main difficulty in identifying the exact moment of formation of EWD is due to the shortage of observed data over the tropical oceans. Some studies have shown that EWDs start over the Africa western coast and intersect the south-equatorial Atlantic basin reaching the South America coast [27, 30], most likely induced through the meridional shift of the ITCZ [47]. Other studies have suggested that EWDs may also be linked to the displacement of cold fronts to lower latitudes [27]. This shows the necessity of studies on the possible interactions of EWD to provide a better understand of their life cycle.

In an attempt to indicate the preferred areas that EWDs occur, including their genesis, and lysis, spatial statistics of the detected EWD (Figure 11) were determined using

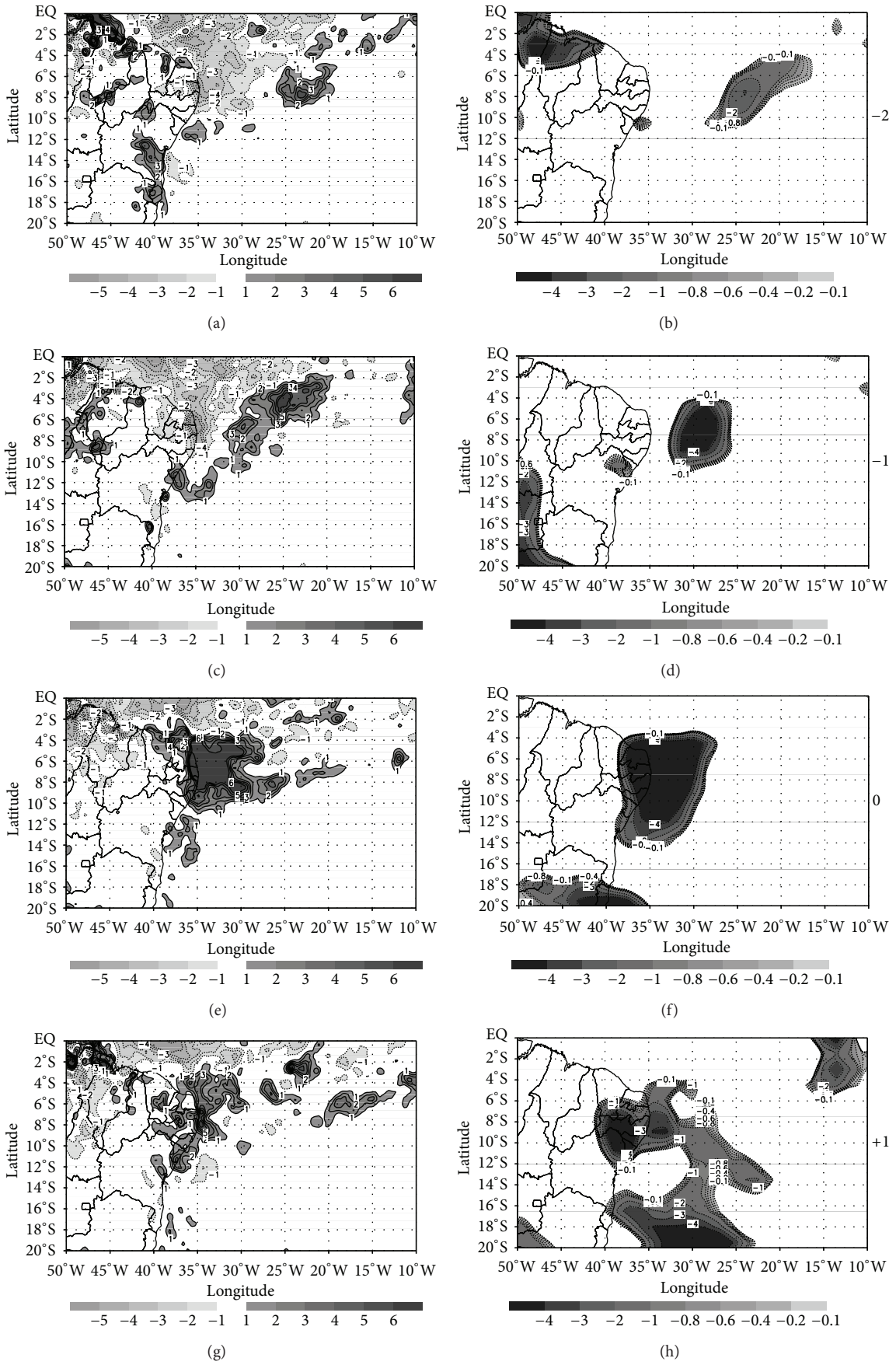

Figure 9: Continued.

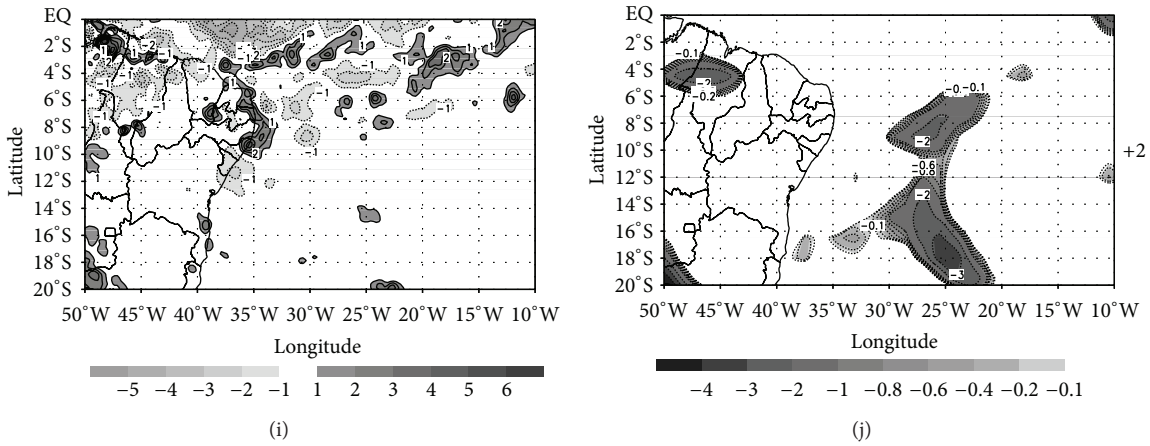

Figure 9: Precipitation (left column, mm·day^{-1}) and outgoing longwave radiation (right column, W·m^{-2}) composite anomalies in the period from April to July 2007.

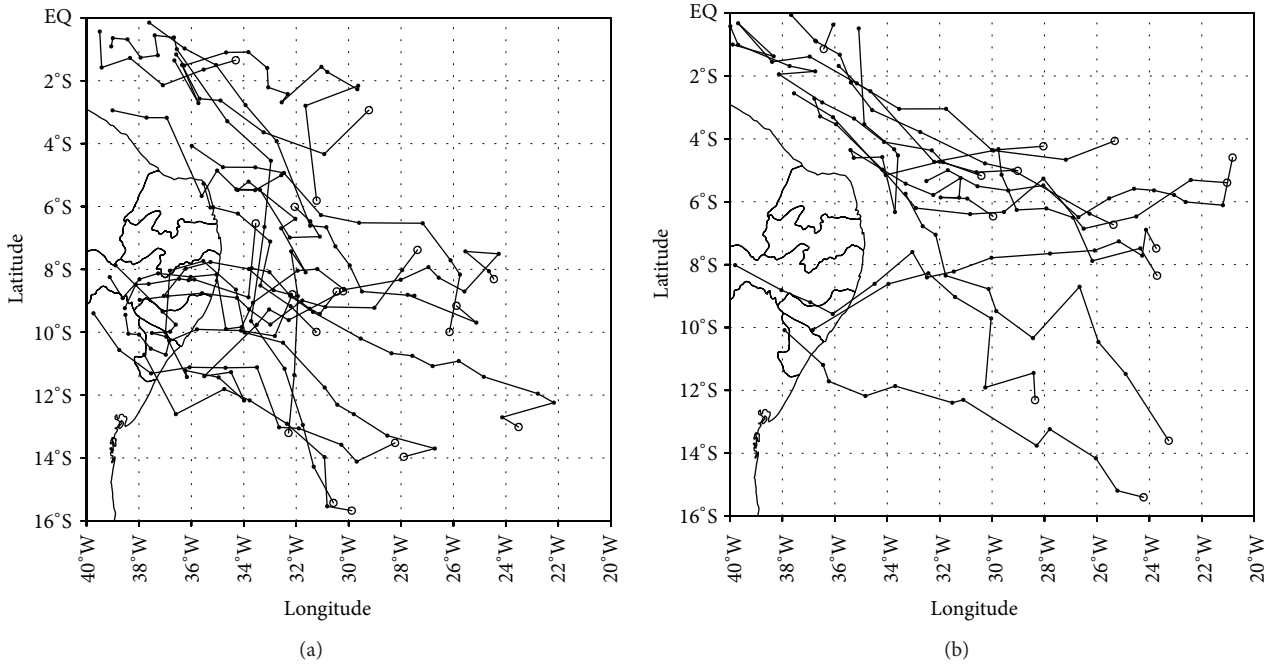

Figure 10: Cyclonic vorticity centres tracks for April–July 2006 (a) and 2007 (b) at 850 hPa.

the vorticity centers detected by TracKH for the 2006 (19 events) and 2007 (15 events) rainy seasons. These results are preliminary due to the low numbers of detected EWD and a longer analysis using more years will provide more definitive results.

The 850 hPa genesis density based on the 2006 (Figure 11(a)) and 2007 (Figure 11(d)) periods show those regions where the tracked systems are first identified. The genesis regions seem to indicate some evidence of the propagation of EWDs over the tropical south Atlantic according to [48]. In 2006, two maxima were observed near ENEB (10°S, 25°W) and northern NEB coast (2°N, 40°W). In the 2007 season, in contrast, there is a continuous belt extending from about 15°S–15°W to 5°N–45°W. Also observed, over the TSA, is the existence of other favorable regions of genesis in both periods. Several tracks can be seen to start from this region in Figures 10(a) and 10(b). Based on the observational analysis of satellite images, streamlines, and cyclonic vorticity, the study of [31] identified the regions of EWDs genesis and dissipation for the 2006 to 2010 rainy seasons over the ENEB. The results were similar to those obtained by TrackH but with genesis shifted to the central TSA. This is probably due to the detection criteria used by the tracking technique and possibly also the quality of the reanalyses in terms of resolution and the observations assimilated. The track density shows a well-defined belt close to the NEB eastern and northern coast during the 2006 rainy season (Figure 11(b)). In 2007 (Figure 11(e)),

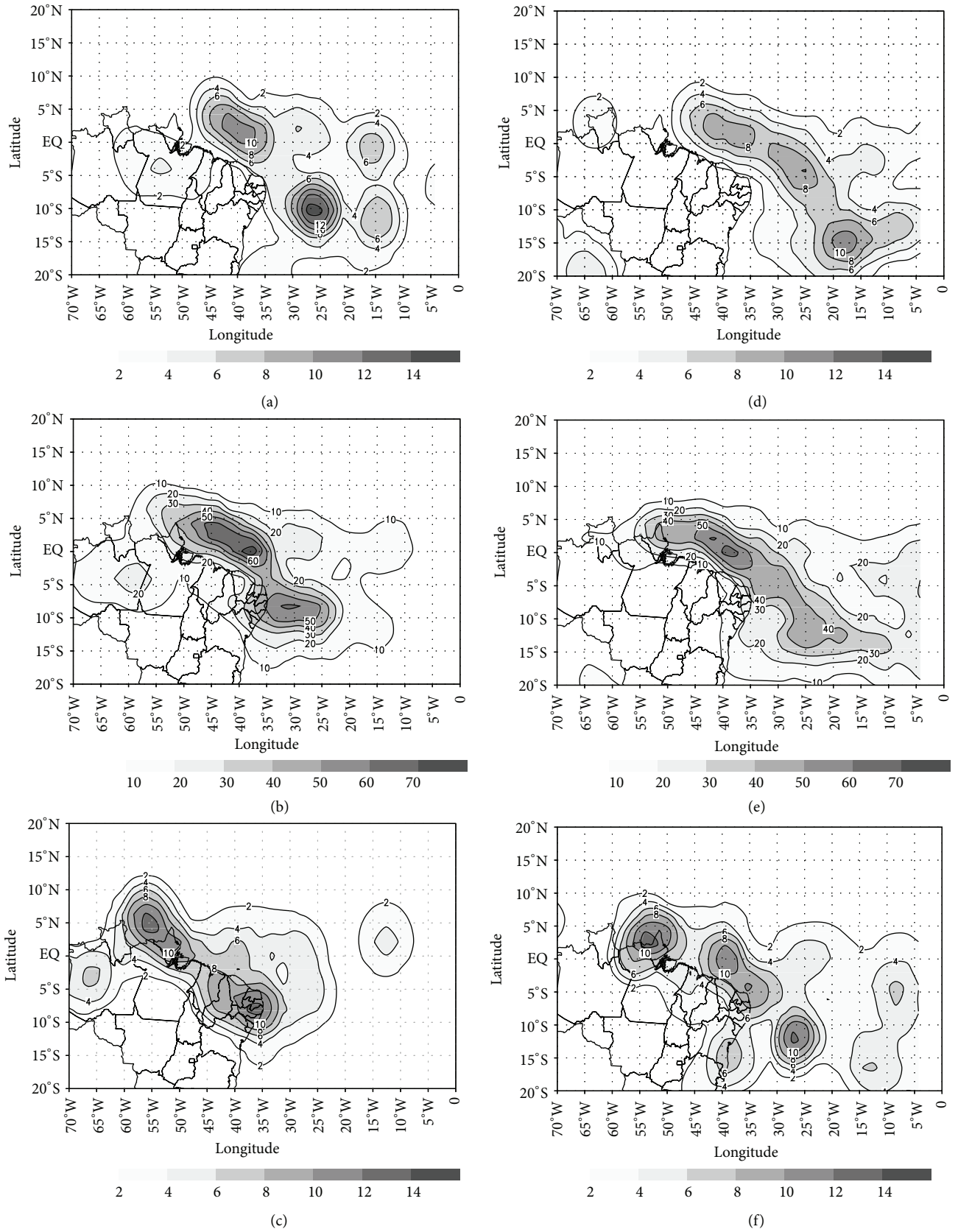

Figure 11: Tracking statistics at 850 hPa to the rainy season (AMJJ) of 2006 (left column) and 2007 (right column). ((a), (d)) Genesis density scaled to number density per unit area (~10^6 km^2) per season, shading indicates values greater than 6. ((b), (e)) Track density per unit area (~10^6 km^2) per season, shading indicates values greater than 40. ((c), (f)) Lysis density per unit area (~10^6 km^2) per season, shading values are the same as in ((a), (d)).

the tracks start over the central TSA (~13°S, 20°W) and stretch westward over the South America northern coast. These results agree with the spatial distribution of individual trajectories tracked and presented in Figure 10. The study of [30] investigated ocean-atmosphere phenomena that could be related to strong rainfall episodes over the eastern NEB during the rainy season of a three-year period (2004–2006). Their results indicated that a significant percent of such strong rainfall episodes were associated with EWDs/positive vorticity anomalies at 700 hPa, which initiate east of 20°W and propagate westward, reaching the ENEB.

The preferred regions of EDWs lysis at 850 hPa are shown in Figure 11(c) (2006) and Figure 11(f) (2007). The striking feature in both periods is the predominance of lysis near the ENEB. In the 2007 season, one can still highlight a greater spatial distribution of lysis compared to 2006 and is similar to the results of Figures 11(a) and 11(d).

From the objective analysis we observe that the method to identify and track EWDs detects about 73% (68%) of the 26 (22) observed events in 2006 (2007), indicating a very promising technique for tracking of these systems over this region. The information about the EWDs life cycle was also obtained. For their genesis, we highlight the mean between 20°–15°W (longitude) and 20°S–5°N (latitude) region while the trajectory and dissipation occur mainly near the ENEB.

4. Summary and Conclusions

The circulation patterns generated by the occurrence of EWDs propagating to the ENEB eastern coast and their importance for the total rainfall over this region during the 2006 and 2007 rainy seasons has been evaluated in detail by a composite analysis using the ERA-Interim data. The choice of these two years, within the period of five years considered in the study of [31], was chosen to evaluate the variability from one year with EWDs events with less convective activity (2006) against a year with more convective activity (2007). The composites were computed from two days before (−2 d) until two days after (+2 d) the EWDs occurred at the coast. In addition, the life cycle of these disturbances has been investigated using an automatic objective analysis method.

The EWD mean characteristics for the two rainy seasons (2006-2007) were estimated using satellite images and composite fields. The EWDs presented an average of 5 days' duration between detection (TSA) and dissipation (NEB) according to the satellite images. Using the 700 hPa composite fields, the EWD average lifetime and wavelength are 5.5 days and 4500 km (45°), respectively. The mean phase velocity was 9.5 m s^{-1} for the same period.

The synoptic analysis of the composites showed a well-organized structure at low levels (1000–700 hPa) in both rainy seasons. The anomalies presented a cyclonic vorticity, convergence/divergence, and wind anomalies associated with EWDs at all levels from two days before, whilst over the TSA, until the day that EWDs reach the ENEB. Another important feature identified in both seasons is the horizontal convergence between 1000–850 hPa superimposed on a divergence pattern at 700 hPa. This shows that there may be a convergence/divergence pattern between 1000–700 hPa linked to most of the EWD events. According to [20], the propagation of EWDs is associated with mass convergence (divergence) in the low (medium/high) levels of the atmosphere. The precipitation and OLR anomalies indicate the convection and precipitation associated with EWDs through the two seasons, with a higher intensity and greater convective activity in 2007 compared to the 2006 season.

The atmosphere vertical structure associated with EWDs was investigated by vertical cross-section composite anomalies of relative humidity, vertical velocity and temperature. The propagation of EWDs to the ENEB was associated with centres of moist and upward motion from two days before reaching ENEB until the systems reach the ENEB, as seen in the horizontal structure analysis. However, during the 2007 rainy season these patterns were observed until day +2 d. The temperature was associated with negative (positive) anomalies at low and high (medium) levels of the atmosphere in both seasons.

From the results obtained using TracKH it was possible to have a better understanding of the life cycle of EWDs, such as the preferred regions for genesis, track, and lysis which identified preferred regions in 2006, one near the eastern NEB (10°S, 25°W) coast and another near the northern NEB (5°N, 40°W) coast. During the 2007 rainy season a continuous belt was observed extending from about 15°S–15°W to 5°N–45°W. The tracks of these systems can be seen over all ENEB, especially between SE and MA states (defined in Figure 1), as well as their lysis between the NEB coast (northern and eastern) and a few kilometers into the continent. The TracKH managed to capture 71% of EWDs in all periods, indicating that the automatic objective analysis is a promising method to identify and track these waves in the TSA. However, of the total events tracked, 43% of these are EWD and 57% represent relative vorticity centers associated with other types of system, very likely due to the disturbances generated along the trades. This motivates the need for objective criteria to better separate the EWDs from other identified systems.

This study was conducted only for the 2006 and 2007 rainy season. Thus, a further investigation is required to obtain a better understanding of these systems, their dynamics and synoptic processes throughout the year, for example, the calculation of climatologies. To do this, a modification to the tracking scheme, as used in [22] using the vertical average of vorticty and higher resolution, may help to improve the tracking of these systems and reduce the false positive identification. This will be reported in a future paper. We will also evaluate the contribution of EWDs over NEB region in future climate scenarios and contrast it with their current distribution.

Conflict of Interests

The authors declare that there is no conflict of interests regarding the publication of this paper.

Acknowledgments

This study was supported by Conselho Nacional de Desenvolvimento Científico e Tecnólogico, CNPq (Grant nos.

143207/2009-1 and 304298/2014-0) and Fundação de Amparo à Pesquisa do Estado de São Paulo, FAPESP, Brazil (Grant no. 08/58101-9).

References

[1] V. E. Kousky and P. S. Chu, "Fluctuation in annual rainfall for Northeast Brazil," *Journal of the Meteorological Society of Japan*, vol. 56, pp. 457–465, 1978.

[2] V. E. Kousky, "Frontal influences on northeast Brazil," *Monthly Weather Review*, vol. 107, no. 9, pp. 1140–1153, 1979.

[3] V. B. Rao, M. C. de Lima, and S. H. Franchito, "Seasonal and interannual variations of rainfall over eastern northeast Brazil," *Journal of Climate*, vol. 6, no. 9, pp. 1754–1763, 1993.

[4] D. M. G. D. Strang, "Climatological analysis of rainfall normals in Northeast Brazil," Centro Tecnológico Aeroespacial (IAE-M 02/72), 1972.

[5] S. Hastenrath and L. Heller, "Dynamics of climatic hazards in northeast Brazil," *Quarterly Journal of the Royal Meteorological Society*, vol. 103, no. 435, pp. 77–92, 1977.

[6] V. E. Kousky, "Diurnal rainfall variation in Northeast Brazil," *Monthly Weather Review*, vol. 108, no. 4, pp. 488–498, 1980.

[7] N. J. Ferreira, C. S. Chan, and P. Satyamurti, "Análise dos distúrbios ondulatórios de leste sobre o Oceano Atlântico Equatorial Sul," in *XI Congresso Brasileiro de Meteorologia*, pp. 462–466, Rio de Janeiro, Brazil, 1990.

[8] Y. Yamazaki and V. B. Rao, "Tropical cloudiness over South Atlantic ocean," *Journal of Meteorological Society Japan*, vol. 55, pp. 205–207, 1977.

[9] V. B. Rao, M. C. De Lima, and S. H. Franchito, "Seasonal and interannual variations of rainfall over eastern northeast Brazil," *Journal of Climate*, vol. 6, no. 9, pp. 1754–1763, 1993.

[10] G. J. Alaka and E. D. Maloney, "The influence of the MJO on upstream precursors to African easterly waves," *Journal of Climate*, vol. 25, no. 9, pp. 3219–3236, 2012.

[11] C. L. Bain, K. D. Williams, S. F. Milton, and J. T. Heming, "Objective tracking of African Easterly Waves in Met Office models," *Quarterly Journal of the Royal Meteorological Society*, vol. 140, pp. 47–57, 2014.

[12] G. Berry, C. Thorncroft, and T. Hewson, "African easterly waves during 2004—analysis using objective techniques," *Monthly Weather Review*, vol. 135, no. 4, pp. 1251–1267, 2007.

[13] R. W. Burpee, "The origin and structure of easterly waves in the lower troposphere of North Africa," *Journal of the Atmospheric Sciences*, vol. 29, no. 1, pp. 77–90, 1972.

[14] T. N. Carlson, "Some remarks on african disturbances and their progress over the tropical atlantic," *Monthly Weather Review*, vol. 97, no. 10, pp. 716–726, 1969.

[15] C. D. Hopsch, C. D. Thorncroft, K. I. Hodges, and J. Aiyyer, "West African storm tracks and their relationship to atlantic tropical cyclones," *Journal of Climate*, vol. 20, pp. 2468–2483, 2007.

[16] M. A. Janiga and C. D. Thorncroft, "Regional differences in the kinematic and thermodynamic structure of African easterly waves," *Quarterly Journal of the Royal Meteorological Society*, vol. 139, no. 675, pp. 1598–1614, 2013.

[17] Y. K. Kouadio, L. A. Machado, and J. Servain, "Tropical atlantic hurricanes, easterly waves, and west african mesoscale convective systems," *Advances in Meteorology*, vol. 2010, Article ID 284503, 13 pages, 2010.

[18] T. N. Krishnamurti, *Tropical Meteorology*, WMO Publication No. 364, Compendium of Meteorology, 1978.

[19] K. D. Leppert II, W. A. Petersen, and D. J. Cecil, "Electrically active convection in tropical easterly waves and implications for tropical cyclogenesis in the atlantic and east pacific," *Monthly Weather Review*, vol. 141, no. 2, pp. 542–556, 2013.

[20] R. J. Reed, D. C. Norquist, and E. E. Recker, "The structure and properties of African wave disturbances as observed during phase III of GATE," *Monthly Weather Review*, vol. 105, no. 3, pp. 317–333, 1977.

[21] H. Riehl, *Tropical Meteorology*, McGraw-Hill, 1954.

[22] Y. L. Serra, G. N. Kiladis, and K. I. Hodges, "Tracking and mean structure of easterly waves over the Intra-Americas Sea," *Journal of Climate*, vol. 23, no. 18, pp. 4823–4840, 2010.

[23] C. D. Thorncroft, "An idealized study of African easterly waves. III. More realistic basic states," *Quarterly Journal of the Royal Meteorological Society*, vol. 121, no. 527, pp. 1589–1614, 1995.

[24] C. Thorncroft and K. Hodges, "African easterly wave variability and its relationship to Atlantic tropical cyclone activity," *Journal of Climate*, vol. 14, no. 6, pp. 1166–1179, 2001.

[25] M.-L. C. Wu, O. Reale, and S. D. Schubert, "A characterization of African easterly waves on 2.5–6-day and 6–9-day time scales," *Journal of Climate*, vol. 26, no. 18, pp. 6750–6774, 2013.

[26] E. D. Coutinho and G. Fisch, "Distúrbios ondulatórios de leste (DOLs) na região do centro de lançamento de Alcântara-MA," *Revista Brasileira de Meteorologia*, vol. 22, no. 2, pp. 193–203, 2007.

[27] A. Diedhiou, L. A. Machado, and H. Laurent, "Mean kinematic characteristics of synoptic easterly disturbances over the Atlantic," *Advances in Atmospheric Sciences*, vol. 27, no. 3, pp. 483–499, 2010.

[28] B. A. Hall, "Westward-moving disturbances in the South Atlantic coinciding with heavy rainfall events at Ascension Island," *Meteorological Magazine*, vol. 118, no. 1405, pp. 175–181, 1989.

[29] M. T. Kayano, "Low-level high-frequency modes in the Tropical Atlantic and their relation to precipitation in the equatorial South America," *Meteorology and Atmospheric Physics*, vol. 83, no. 3-4, pp. 263–276, 2003.

[30] Y. K. Kouadio, J. Servain, L. A. T. MacHado, and C. A. D. Lentini, "Heavy rainfall episodes in the eastern northeast brazil linked to large-scale ocean-atmosphere conditions in the tropical atlantic," *Advances in Meteorology*, vol. 2012, Article ID 369567, 16 pages, 2012.

[31] B. F. Pontes da Silva, *Contribuição dos Distúrbios Ondulatórios de Leste para a Chuva no Leste do Nordeste do Brasil: Evolução Sinótica Média e Simulações Numéricas [Dissertação]*, Universidade de São Paulo, Instituto de Astronomia, Geofísica e Ciências Atmosféricas, Departamento de Ciências Atmosféricas, 2011.

[32] R. R. Torres and N. J. Ferreira, "Case studies of easterly wave disturbances over Northeast Brazil using the Eta Model," *Weather and Forecasting*, vol. 26, no. 2, pp. 225–235, 2011.

[33] A. Simmons, S. Uppala, and D. P. Dee, "Update on ERA-interim," *ECMWF Newsletter*, vol. 111, no. 5, 2007.

[34] A. Simmons, S. Uppala, D. P. Dee, and S. Kobayashi, "ERA-interim: new ECMWF reanalysis products from 1989 onwards," *ECMWF Newsletter*, vol. 110, pp. 25–35, 2007.

[35] S. Uppala, D. Dee, S. Kobayashi, P. Berrisford, and A. Simmons, "Towards a climate data assimilation system: status update of ERA-Interim," *ECMWF Newsletter*, vol. 115, pp. 12–18, 2008.

[36] D. P. Dee, S. M. Uppala, A. J. Simmons et al., "The ERA-Interim reanalysis: configuration and performance of the data assimilation system," *Quarterly Journal of the Royal Meteorological Society*, vol. 137, no. 656, pp. 553–597, 2011.

[37] B. Liebman and C. A. Smith, "Description of a complete (interpolated) outgoing longwave radiation dataset," *Bulletin of the American Meteorological Society*, vol. 77, pp. 1275–1277, 1996.

[38] G. J. Huffman, R. F. Adler, M. M. Morrissey et al., "Global precipitation at one-degree daily resolution from multisatellite observations," *Journal of Hydrometeorology*, vol. 2, no. 1, pp. 36–50, 2001.

[39] K. I. Hodges, "Feature tracking on the unit sphere," *Monthly Weather Review*, vol. 123, no. 12, pp. 3458–3465, 1995.

[40] K. I. Hodges, "Adaptive constraints for feature tracking," *Monthly Weather Review*, vol. 127, no. 6, pp. 1362–1373, 1999.

[41] G. C. Asnani, *Tropical Meteorology*, Noble Printers, Pune, India, 1993.

[42] L. Bengtsson, K. I. Hodges, and M. Esch, "Tropical cyclones in a T159 resolution global climate model: comparison with observations and re-analyses," *Tellus, Series A: Dynamic Meteorology and Oceanography*, vol. 59, no. 4, pp. 396–416, 2007.

[43] K. I. Hodges, "Spherical nonparametric estimators applied to the UGAMP model integration for AMIP," *Monthly Weather Review*, vol. 124, no. 12, pp. 2914–2932, 1996.

[44] E. S. Espinosa, *Distúrbios nos Ventos de Leste no Atlântico Tropical [Ph.D. dissertation]*, Instituto Nacional de Pesquisas Espaciais, São Paulo, Brazil, 1996.

[45] G. V. Mota and A. W. Gandu, "Análise dos Padrões Ondulatórios de Leste no Nordeste Brasileiro Durante o Inverno de 1994," in *X Congresso Brasileiro de Meteorologia*, Brasília, Brazil, 1998.

[46] E. S. Merritt, "Easterly waves and perturbations, a reappraisal," *Journal of Applied Meteorology*, vol. 3, no. 4, pp. 367–382, 1964.

[47] R. H. Simpson, N. Frank, D. Shideler, and H. M. Johnson, "Atlantic tropical disturbances, 1967," *Monthly Weather Review*, vol. 96, no. 4, pp. 251–259, 1968.

[48] F. A. Berry, E. Bollay, and N. R. Beers, *Handbook of Meteorology*, McGraw-Hill, New York, NY, USA, 1945.